



Amphiphilic perfluoroalkyl carbohydrates as new tools for liver imaging

C. Richard^{a,b,c,d}, P. Chaumet-Riffaud^{e,f}, A. Belland^{a,b,c,d}, A. Parat^g, C. Contino-Pepin^g, M. Bessodes^{a,b,c,d}, D. Scherman^{a,b,c,d}, B. Pucci^g, N. Mignet^{a,b,c,d,*}

^a Unité de Pharmacologie Chimique et Génétique, CNRS, UMR 8151, Paris, F-75270 cedex, France

^b Inserm, U 640, Paris, F-75270 cedex, France

^c Université Paris Descartes, Faculté des Sciences Pharmaceutiques et Biologiques, Paris, F-75270 cedex, France

^d ENSCP, Paris, F-75231 cedex, France

^e Université Paris-Sud, EA4046, UFR de Bicêtre, Le Kremlin-Bicêtre, F-94275, France

^f AP-HP, CHU de Bicêtre, Service de Biophysique et de Médecine nucléaire, F-94275, France

^g Laboratoire de Chimie Bioorganique et des Systèmes Moléculaires Vectoriels, Université d'Avignon, Avignon, F-84000, France

ARTICLE INFO

Article history:

Received 30 January 2009

Received in revised form 9 April 2009

Accepted 18 May 2009

Available online 6 June 2009

Keywords:

Galactosylated amphiphiles

Perfluoroalkyl surfactants

Radiolabeled particles

Hepatocyte targeting

Liver scintigraphy

ABSTRACT

The synthesis of three molecules containing a fluorocarbon chain (either C₆F₁₃, C₈F₁₇ or C₁₀F₂₁), a sugar moiety (derived from lactobionic acid) and a chelate (derived from DTPA) is reported. These molecules (C₆F₁₃-Gal-DTPA, C₈F₁₇-Gal-DTPA or C₁₀F₂₁-Gal-DTPA) have been dispersed in water and their critical micellar concentration (CMC) as well as their size were determined. Their interaction with serum was weak as evaluated by time resolved fluorimetry of europium complexes. The presence of sugar on the surface of the nanoparticles was confirmed by the agglutination test using ricin. Conditions of pH and concentrations were optimised for *in vivo* studies. Finally, the nanoparticles formed with C₁₀F₂₁-Gal-DTPA have been complexed with ^{99m}Tc and injected to rats in order to follow their biodistribution by scintigraphy while following their stability by transmission electronic microscopy. A majority of the compound was found in the liver post-bolus injection.

© 2009 Elsevier B.V. All rights reserved.

1. Introduction

The quantification of the hepatic functional reserve (HFR) has demonstrated its clinical utility for optimising the medical care of liver disorders (prognosis, staging, diagnosis, post-surgery follow-up) (Hwang et al., 1999; Abe et al., 2003). Currently, the quantitative measurement of the HFR is not performed in Europe where hepatic function is indirectly evaluated by biochemical dosages of enzymatic activity and/or metabolites (Child and Turcotte, 1964; Pugh et al., 1973; Bedossa and Poynard, 1996; Imbert-Bismut et al., 2001).

The mammalian asialoglycoprotein receptors (ASGPR) are mainly located on the hepatocyte sinusoidal membrane. The ASGPR bind and endocytose asialoglycoproteins (galactosylated proteins). Quantitative imaging of the ASGPR density estimates liver function, thus allowing non-invasive and quantitative assessment of the functioning hepatocytes in many liver diseases. Liver scintigraphy with radiolabeled ASGPR ligands has already proved to be useful in monitoring the native and grafted liver functions in patients who

had undergone orthotopic liver transplantation. A specific marker of the ASGPR has been prepared, its liver uptake depends mainly on the ASGPR density rather than on the hepatic blood flow (Jeong et al., 2004). This radiopharmaceutical is exclusively distributed in Japan and this diagnostic tool is lacking in Europe to assess hepatic functional reserve in transplanted patients. However, importation is very unlikely in France, because of the origin of the raw material, human albumin, and of the lack of harmonized safety requirements between France and Japan. Moreover their chemical procedure involves cyanide derivatives (amidation using cyanomethyl-1-thioglycosides), which could raise registration issues in France.

We have recently described an original synthetic process for a modified human albumin bearing lactosyl ligands and technetium-chelating sites (DTPA) (Scherman et al., 2008). Initial preclinical studies enabled us to characterize the product and to conduct biodistribution studies in two murine species. These results further support its use in clinical imaging. Although human serum albumin is a component of many pharmaceutical preparations (Pulmocis[®], Technescan LyoMAA[®]), the use of human serum albumin might not represent the optimal choice in terms of safety concerns. Indeed, the use of human albumin from donors requires strict follow-up, and informing the patient about the potential risks associated to the injection of blood derived products. Hence, we decided to focus our research on non-protein derivatives.

* Corresponding author at: Unité de Pharmacologie Chimique et Génétique, CNRS, UMR 8151, Paris, F-75270 cedex, France. Tel.: +33 153 739 581; fax: +33 143 266 918.
E-mail address: Nathalie.Mignet@univ-paris5.fr (N. Mignet).

Glycolipids received considerable attention for their involvement in a variety of physiological events (Hakomori and Handa, 2000) as well as their surfactant properties which have led to numerous industrial applications (Von Rybinski and Hill, 1998). Moreover, thanks to their polar head group, carbohydrate amphiphiles are likely to bind membrane lectins: in this case, their lipid moiety is expected to provide a cluster effect through self-association (Arya et al., 1999; Coulon et al., 1998; Sliedregt et al., 1999). Many synthetic efforts have been devoted to the preparation of sophisticated polar headgroups or lipidic tails conferring to the amphiphile optimised binding properties (Chabaud et al., 1998) or absence of detergency toward cell membranes (Maurizis et al., 1993). Thus the introduction of a fluoroalkyl chain instead of a classical hydrocarbon one as hydrophobic part of the glycosylated surfactant minimizes the cell toxicity of such amphiphilic molecules (Chabaud et al., 1998). Indeed, it is well known that hydrocarbon and fluorocarbon chains exhibit poor miscibility, avoiding the mixing of fluorocarbon surfactants and phospholipids of the biological membranes (Chabaud et al., 1998; Barthélémy et al., 2002). Moreover, for a given type of polar head, fluorocarbon surfactants tends to exhibit a markedly lower CMC and form structures with less interfacial curvature than hydrocarbon ones. Thus, they usually form cylindrical micelles, rod-like or disc assemblies (10–50 nm) as already reported for ammonium perfluorooctanoate, cationic, polyoxyethylene, lactose or maltose-derived fluorosurfactants (Kissa, 1994; Ravey et al., 1994; Burkitt et al., 1987; Wang et al., 1999; Lebaupain et al., 2006; Polidori et al., 2006). According to these previous results, a fluorinated carrier including a lysine moiety was designed endowed with a lactobionamide group as a hydrophilic head and a fluorinated chain as hydrophobic part, its ϵ -amino group allowing the anchorage of either an active principle, a cryptand group or other residues (Périno et al., 2006).

As reaching via the hepatocytes via the intersinusoidal space calls for very small structures, we assumed that lactosylated fluorinated surfactants could be good candidates to the design of new, non-proteic probes for hepatocyte imaging. We report herein the synthesis of amphiphilic perfluoroalkyl carbohydrates modified with DTPA, their physicochemical properties and their use *in vivo* as possible hepatocyte scintigraphic imaging agents.

2. Materials and methods

2.1. Materials

Diethylenetriaminepentaacetic dianhydride (DTPA dianhydride) was purchased from Aldrich. The solvents were from Carlo Erba-SDS and were used without further purification. F-SPE cartridges were obtained from Aldrich. ^1H , ^{13}C and ^{19}F NMR spectra were performed on a Bruker DRX400 operating at 400, 100 and 376.32 MHz, respectively. MS were carried out on a Shimadzu 2010A LC-MS on ESI mode. The size of the particles was determined using a Zeta Nanosizer from Malvern Instruments, France. Critical micellar concentrations were determined using Krüss K100 tensiometer. *Ricinus Communis Agglutinin* (RCA120) and serum were purchased from Sigma. Time resolved fluorimetry and lectin aggregation tests were performed on a Wallac Victor2 1420 Multilabel Counter from PerkinElmer. Rats (male Wistar, 270 g) were purchased from Elevage Janvier, France. Biodistribution studies were done using a small-animal dedicated gamma camera (BIOSPACE, France; low energy high resolution parallel collimator, FOV 8 cm). Radio-TLC chromatograms were obtained using a raytest miniGITA imaging system. A gamma scintillation counter Wizard 1480 automatic model from PerkinElmer Company was used to count the radioactivity of rat organs in the biodistribution studies.

2.2. Synthesis of perfluoroalkyl carbohydrate amphiphiles

2.2.1. Synthesis of compound 2

Compound **1** (2.2×10^{-4} mol, 287.71 mg for $n=6$) was dissolved in 10 mL of a ethanol/acetic acid solution (99/1, v/v) at 0 °C, then 0.013 g of 10% Pd/C was slowly added. The reaction mixture was submitted to a hydrogen atmosphere for 2 h (7 bars). After filtration of the catalyst through a pad of celite and evaporation of the solvent in vacuo, compound **2** was obtained as yellow powders ($n=6$: 98% yield; $n=8$: 99% yield; $n=10$: 94% yield).

2.2.1.1. Analyses for C_6F_{13} -Gal(OAc). ^1H NMR (CDCl_3): δ (ppm) 7.8–7.7 (2H, m, NH); 5.5 (1H); 5.30–5.38 (2H, m); 4.98–5.18 (3H, m); 4.5–4.58 (2H, d); 4.35–3.9 (6H, m); 3.52 (2H, m, CH_2NH); 2.95 (2H, t, CH_2NH); 2.45–1.78 (26H, m, CH_2CF_2 , CH_3 -COO); 1.75–1.28 (6H, m, CH_2 -Lys).

^{13}C NMR (CDCl_3): δ (ppm) 177.1; 173.8; 169.2; 167.9; 101.5; 78.1; 70.7; 70.53; 70.48; 69.9; 69.3; 69.0; 68.8; 66.6; 61.3; 60.8; 51.9; 38.9; 31.6; 30.9; 30.8; 29.1; 26.2; 21.6 à 20.3.

^{19}F NMR (CDCl_3): δ (ppm) –80.0; –113.5; –121.1; –122; –122.8; –125.3.

2.2.1.2. Analyses for C_8F_{17} -Gal(OAc). ^1H NMR (CDCl_3): δ (ppm) 8.20 (3H, NH_2 , NH); 8.05 (1H, NH); 4.47–4.42 (1H); 5.21–5.28 (2H, m); 5.20–4.90 (3H, m); 4.6–4.4 (2H); 4.4–3.9 (6H, m); 3.47 (2H, m, CH_2NH); 2.9 (2H); 2.3 (2H, CH_2 -Lys); 2.22–1.9 (26H, m, CH_2CF_2 , CH_3 -COO); 1.65 (4H, m, CH_2 -Lys).

^{13}C NMR (CDCl_3): δ (ppm) 177.2; 171.2; 168.7; 167.2; 101.1; 72.1; 70.3; 69.5; 69.4; 68.9; 68.6; 68.5; 68.4; 66.3; 60.9; 60.4; 50.5; 38.4; 31.2; 29.8; 25.9; 22.9; 21.4; 21.3 à 18.3.

^{19}F NMR (CDCl_3): δ (ppm) –80.0; –113.4; –121.0; –121.9; –122.8; –125.3.

MS: m/z = 1268 ($[\text{M}+\text{H}]^+$).

2.2.1.3. Analyses for $\text{C}_{10}\text{F}_{21}$ -Gal(OAc). ^1H NMR (CDCl_3): δ (ppm) 7.9–7.5 (2H, m, NH); 5.38 (1H); 5.3–5.1 (3H, m); 5.1–4.85 (9H, m); 4.45 (2H); 4.25 (1H); 4.1 (2H, m); 3.9 (2H, m); 3.8 (1H, m); 3.4 (2H, m, CH_2NH); 2.8 (2H); 2.15–1.75 (26H, m, CH_2CF_2 , CH_3 -COO); 1.6–1.1 (6H, m, CH_2 -Lys).

^{19}F NMR (CDCl_3): δ (ppm) –80.8; –114.2; –121.8; –122.7; –123.6; –126.2.

MS: m/z = 1368 ($[\text{M}+\text{H}]^+$).

2.2.2. Synthesis of compound 3

Compound **2** (1.06×10^{-4} mol, 133.9 mg for $n=6$) was dissolved in anhydrous DMF (810 μL) and anhydrous triethylamine (275 μL) was then added dropwise. This solution was then added via a syringe to a solution of diethylenetriaminepentaacetic acid dianhydride (DTPA-dianhydride) (191 mg, 5.35×10^{-4} mol) dissolved in anhydrous DMF (2.5 mL) under argon. This solution was then stirred for 4 h. In the case of $n=8$ and $n=10$ the reaction was stirred overnight. H_2O (14 mL) was then added and the solution was stirred for 2 h. After evaporation of the solvent in vacuo, AcOEt (10 mL) was added to precipitate the excess of DTPA. The solution was collected and evaporated under vacuum to give a yellow powder (42.6 mg, 2.6×10^{-5} mol). Then F-SPE (fluorous solid phase extraction) cartridge (Curran, 2003) was used to separate non-fluorous compounds (the rest of DTPA which did not precipitate) from the fluorous molecules (compound **3**). Typically, the mixture was first dissolved in anhydrous DMF (400 μL) and loaded onto the F-SPE cartridge. Using first 8 mL of a fluorophobic solvent (MeOH/ H_2O , 80/20), DTPA was eluted from the cartridge. The fluorous compound **3** was then washed off the cartridge using a fluorophilic solvent such as MeOH, acetone or THF. The solvent was then evaporated under vacuum to

give compound **3** ($n=6$: 45% yield; $n=8$: 64% yield; $n=10$: 50% yield).

2.2.2.1. Analyses for C_6F_{13} -Gal(OAc)-DTPA. 1H NMR (DMSO): δ (ppm) 8.4–8.1 (3H, NH); 5.5 (1H); 5.25–5.15 (3H, m); 5.0–4.75 (3H, m); 4.42 (2H, m, CH_2NH); 4.25 (2H, t); 4.2–3.92 (6H, m); 3.6–2.8 (18H, m, DTPA); 2.2–1.8 (26H, m, CH_2CF_2 , CH_3-COO); 1.60–1.15 (6H, m, CH_2-Lys).

^{19}F NMR ($CDCl_3$): δ (ppm) –80.0; –113.5; –121.1; –122.1; –122.8; –125.3.

MS: $m/z = 1544$ ($[M+2H]^+$).

2.2.2.2. Analyses for C_8F_{17} -Gal(OAc)-DTPA. 1H NMR ($CDCl_3$): δ (ppm) 5.78–5.50 (2H, NH); 5.41–5.22 (2H, m); 5.18–4.90 (3H, m); 4.70–4.40 (3H); 4.0–3.90 (2H, m); 3.90–3.0 (18H, m); 3.5–2.85 (18H, DTPA); 2.38–1.85 (18H, m, CH_3); 1.85–1.4 (4H, m, CH_2-Lys).

^{19}F NMR ($CDCl_3$): δ (ppm) –80.0; –113.5; –121.3; –122.1; –122.9; –125.5.

MS: $m/z = 1644$ ($[M+2H]^+$).

2.2.2.3. Analyses for $C_{10}F_{21}$ -Gal(OAc)-DTPA. 1H NMR (CD_3OD): δ (ppm) 5.62 (1H, NH); 5.3–5.1 (2H, NH); 5.1–4.85 (4H, m); 4.6–4.4 (1H, m); 4.15 (1H); 4.1–3.84 (6H); 3.7–3.6 (2H, m); 3.6–3.48 (4H, m); 3.48–3.22 (8H, m); 3.12–2.9 (12H, m); 2.4–2.2 (2H); 2.2–2.0 (5H, m); 2.0–1.85 (15H, m); 1.82 (6H); 1.68–1.5 (2H); 1.5–1.25 (3H).

^{19}F NMR (CD_3OD): δ (ppm) –80.8; –114.2; –121.8; –122.7; –123.6; –126.2.

MS: $m/z = 1743$ ($[M+H]^+$).

2.2.3. Synthesis of compound **4**: C_6F_{13} -Gal-DTPA, C_8F_{17} -Gal-DTPA and $C_{10}F_{21}$ -Gal-DTPA

Compound **3** (12.4 mg, 8×10^{-6} mol) was dissolved in a solution of $NH_3/MeOH$ 7N (1 mL) at $0^\circ C$. This solution was stirred for 15 min at $0^\circ C$ and then for 2 h at room temperature. The reaction mixture was then evaporated under vacuum to give compound **4** as yellow powders ($n=6$: 98% yield; $n=8$: 97% yield; $n=10$: 99% yield).

2.2.3.1. Analyses for C_6F_{13} -Gal-DTPA. 1H NMR (DMSO): δ (ppm) 8.6–7.6 (1H, m, NH); 7.3 (1H, NH); 6.7 (1H, NH); 4.4–4.1 (8H, m); 4.1–3.9 (8H, m); 3.9–2.18 (40H, m).

^{19}F NMR ($CDCl_3$): δ (ppm) –80.0; –113.5; –121.1; –122.1; –122.8; –125.3.

MS: $m/z = 1207$ ($[M+H]^+$).

2.2.3.2. Analyses for C_8F_{17} -Gal-DTPA. 1H NMR (DMSO): δ (ppm) 8.42 (1H); 8.3 (1H); 8.1–7.9 (1H, m); 8.1–7.6 (1H, m); 7.3 (1H); 6.7 (1H); 4.3–4.1 (12H); 4.0–3.9 (7H); 3.68–3.62 (11H); 3.1–2.98 (8H); 2.98–2.9 (4H); 2.9–2.2 (11H).

^{19}F NMR ($CDCl_3$): δ (ppm) –80.0; –113.5; –121.0; –122.1; –122.9; –125.5.

MS: $m/z = 1309$ ($[M+3H]^+$).

2.2.3.3. Analyses for $C_{10}F_{21}$ -Gal-DTPA. 1H NMR (CD_3OD): δ (ppm) 4.45–4.15 (3H, m); 4.15–3.95 (2H, NH); 5.10–4.85 (1H); 3.95–3.75 (1H, m); 3.75–3.35 (13H, m); 3.30–2.84 (19H, m); 2.40–2.10 (2H, m); 1.82–1.55 (8H, m); 1.55–0.95 (9H).

^{19}F NMR (CD_3OD): δ (ppm) –80.8; –114.2; –121.8; –122.7; –123.6; –126.2.

2.3. Physicochemistry

2.3.1. Determination of the critical micellar concentrations (CMC)

The surface activity of surfactants in solution at the air/water interface was determined by Wilhelmy plate technique. The surfactant solution was prepared 12 h prior to the measurements using Milli-Q water (resistivity of $18.2 M\Omega$ cm, surface tension of

72.0 mN/m at $20^\circ C$, pH 6.1). 20 mL of the surfactant solution was taken in a glass cuvette and surface tensions were determined by dilution technique. All measurements were made at $25 \pm 0.5^\circ C$. Other conditions were identical as reported elsewhere (Lebaupain et al., 2006). All the measurements were repeated two or three times. An estimate of the area per molecule, A_{min} , at the interface is also given, as the derived from the surface excess calculated using the Gibbs adsorption isotherm, $\Gamma_{max} = -(1/RT)(d\gamma/d \ln C)$ where Γ_{max} is the surface excess (moles per unit area), R is the universal gas constant, T is the absolute temperature, γ is the surface tension, and C is the surfactant concentration. The A_{min} can be calculated as $A_{min} = 1/(N_A \Gamma_{max})$, where N_A is the Avogadro number.

2.3.2. Determination of the size of the particles by dynamic light scattering

The hydrodynamic particle size distributions and polydispersity of amphiphiles at different concentrations were determined using a He–Ne laser ($\lambda = 633$ nm, 4.0 mW) (Zetasizer Malvern Nano Series). In a typical experiment, a plastic cuvette was filled with 500 μ L samples of each amphiphile at a concentration of 0.5 mM. The experimental run time was 10.0 min. The time-dependent correlation function of the scattered light intensity was measured at a scattering angle of 173° relative to the laser source (backscattering detection). The hydrodynamic radius (R) of the particles was estimated from their diffusion coefficient (D) using the Stokes–Einstein equation, $D = k_B T / 6\pi\eta R$ where k_B is the Boltzmann's constant, T is the absolute temperature, and η is the viscosity of the solvent.

2.3.3. Determination of the homogeneity of the suspension by transmission electronic microscopy

The samples prepared as described above were loaded on a Formvar/carbon copper grid 200 mesh from Agar Scientific and left to dry for 1 min. Uranyl acetate was dropped on the dried sample and left 1 min to stain the samples. Observations were performed on a microscope JEOL, JEM 100S.

2.4. Interaction with serum

The interaction of the nanoparticles formed with $C_{10}F_{21}$ -Gal-DTPA and serum was studied by time resolved fluorimetry. First, the amphiphile was complexed with 1 equiv. of $EuCl_3 \cdot 6H_2O$ per DTPA. Then, the labeled particles (50 μ M, 100 μ L) were incubated in 100% serum (1 mL) for 2 h at $37^\circ C$. Then proteins were precipitated by the addition of acetone (80%) and the supernatant was recovered. In these conditions, no more protein was detectable by reverse light scattering suggesting an efficient precipitation method. The amount of particles left in the supernatant was evaluated by measuring the retarded fluorescence due to the europium ions complexed with DTPA. Time resolved fluorimetry was performed with 1000 pulses/s and a 320 nm excitation. In the period between flashes, fluorescence of the sample was measured at 615 nm, for 400 μ s which allowed the short fluorescence to decay. The amount of the particles corresponding to 100% was directly added to a supernatant free of amphiphile. The level measured in the supernatant was calculated according to this 100%.

2.5. Lectin recognition

The lectin recognition ability was examined by measuring the absorbance resulting from the interaction of nanoparticles with RCA120 lectin. The tests were realized using $C_{10}F_{21}$ -Gal-DTPA at a concentration of 0.5 mM in water. 1, 2, 5 and 10 μ L of the suspension formed in water was diluted with NaCl (150 mM) in order to get a final volume of 200 μ L. 15 μ L of RCA120 (1 mg/mL) was added and the absorbance was measured at 450 nm. For each point, the value of the absorbance of the nanoparticle alone (without RCA120) was

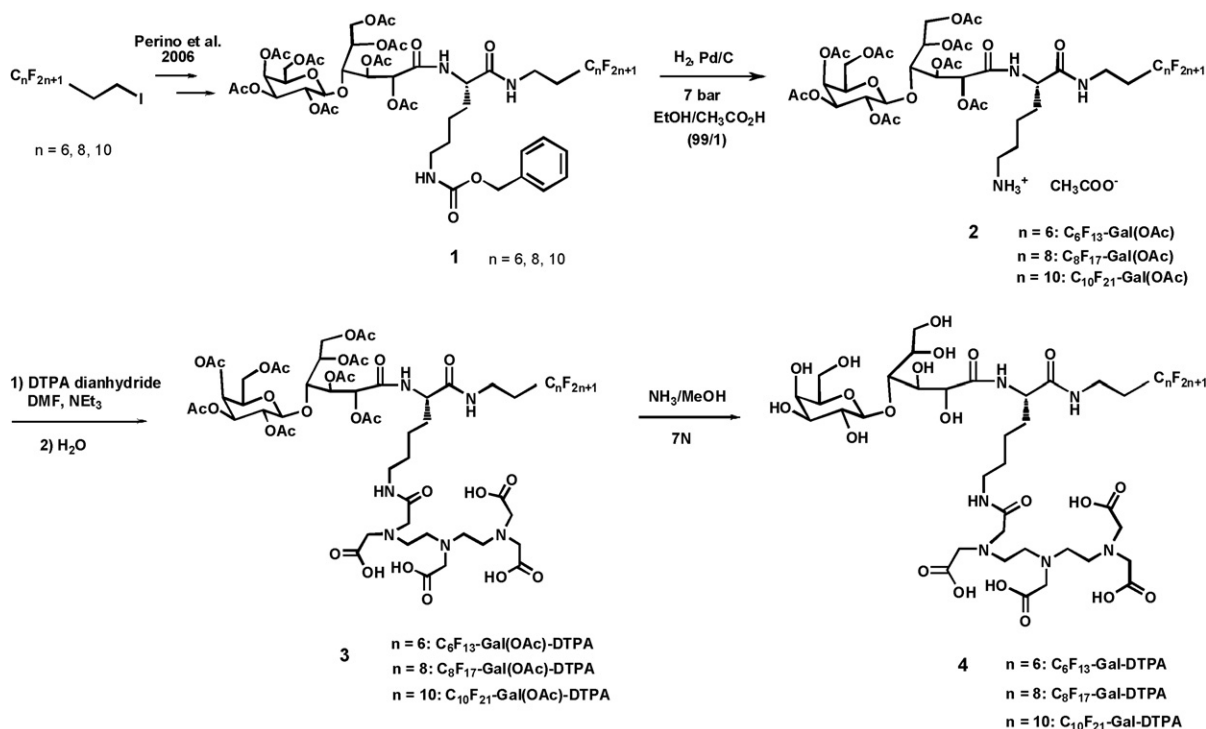


Fig. 1. Synthesis of perfluoroalkylated carbohydrates $C_6F_{13}\text{-Gal-DTPA}$, $C_8F_{17}\text{-Gal-DTPA}$ and $C_{10}F_{21}\text{-Gal-DTPA}$.

subtracted to the value of the absorbance obtained in presence of RCA120. Then, a series of competitive tests was realized using RCA120 preincubated with 20, 40 and 60 μL of lactose (0.1 M). Each assay was carried out in triplicate.

2.6. Optimisation of the conditions for in vivo studies

For pH optimisation, a suspension of $C_{10}F_{21}\text{-Gal-DTPA}$ (200 μM) was prepared by dilution of the sample in sodium acetate (200 mM, pH 6.5). SnCl_2 (50, 200 or 400 μL of a 1 mg/mL solution in HCl 0.1N) was then added to the suspension.

For concentration optimisation, a suspension of $C_{10}F_{21}\text{-Gal-DTPA}$ (50, 100 or 200 μM) was prepared by dilution of the samples in sodium acetate (200 mM, pH 6.5). SnCl_2 (50, 100 or 200 μL of a 1 mg/mL solution in HCl 0.1N) was then added to the suspension.

2.7. Complexation of the nanoparticles with ^{99m}Tc and biodistribution in rats

Suspensions of $C_{10}F_{21}\text{-Gal-DTPA}$ (50, 100 or 200 μM) were prepared in sodium acetate (200 mM) and filtered on 0.22 μm in a sterile environment. SnCl_2 diluted in HCl 0.1N was then added to the suspension. Freshly eluted ^{99m}Tc -pertechnetate, from a 99 molybdenum generator, was added to the suspension (30 MBq per flacon) and incubated at 50 $^\circ\text{C}$ for 30 min. Labeling efficiencies were determined by ITLC chromatography according to Eckelman (ethanol:10% ammonium acetate = 1:1) Eckelman, 1995. Labeling was terminated in 30 min at 50 $^\circ\text{C}$ with >97% efficiency.

Experiments were conducted following NIH recommendation for animal experimentation. Following anesthesia with pentobarbital, Wistar rats were injected intravenously through the penis vein with 200 μL of tracer (5–8 MBq). Acquisition (mode list) was done in the supine position. Dynamic images were acquired over 30 min for all animals and in some cases up to 4 h. Regions of interest (ROIs) were set on the heart and the liver. Animals were sacrificed at the end of acquisitions. The weights and radioactivities of blood, liver,

spleen, lung, and kidney samples excised from the sacrificed rats were measured using an electronic balance and a gamma scintillation counter. Results were expressed as activity per gram of tissue.

3. Results and discussions

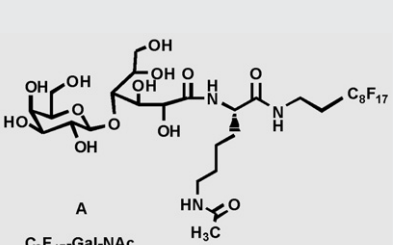
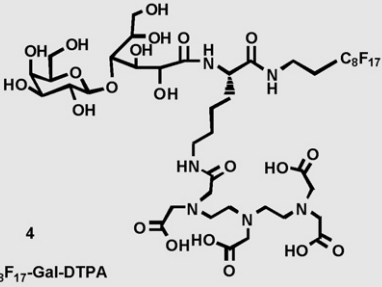
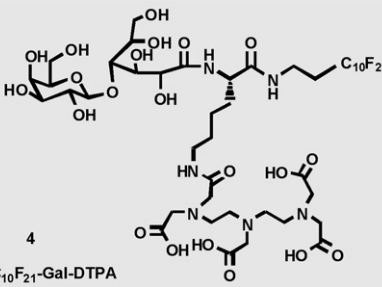
3.1. Syntheses of the molecules

The synthetic scheme of the three perfluoroalkylated carbohydrates $C_nF_{2n+1}\text{-Gal-DTPA}$ ($n=6, 8$ or 10) is outlined in Fig. 1. Compounds **1** prepared as previously described (Périno et al., 2006) (either with $n=6, n=8$ or $n=10$) were first hydrogenated to quantitatively provide the corresponding amine derivatives, which were then reacted with DTPA dianhydride to give compounds **3** in 45–64% yields. Removal of the acetyl protective groups afforded compounds **4** (either $C_6F_{13}\text{-Gal-DTPA}$, $C_8F_{17}\text{-Gal-DTPA}$ or $C_{10}F_{21}\text{-Gal-DTPA}$) in quantitative yields.

3.2. Critical micellar concentrations (CMC)

The surface tensions versus concentration of aqueous solution of compounds $C_8F_{17}\text{-Gal-DTPA}$ and $C_{10}F_{21}\text{-Gal-DTPA}$ were measured. The critical micellar concentration (CMC) value of these compounds was respectively 0.14 and 0.01 mM. Such low values could be ascribed to the presence of the fluorocarbon chain which generally induces a dramatic decrease of the CMC by comparison with hydrocarbon analogues. This high impact of fluoromethylene group on surfactant aggregation behavior is clearly shown by comparing the CMC values measured for $C_8F_{17}\text{-Gal-DTPA}$ and $C_{10}F_{21}\text{-Gal-DTPA}$. One can note that an addition of two fluoromethylene groups on the fluorinated tail induces a decrease of one order of magnitude on the CMC value. Such a behavior once again highlights the impact of fluorinated tail on the aggregation ability of such surfactants. Moreover, the tensiometric curves led us to specify the polar head interfacial cross-sections of compound **4** by applying the

Table 1Critical micellar concentration (CMC) and air–water interfacial cross-sections of surfactant polar head (a) of the compounds C₈F₁₇-Gal-DTPA and C₁₀F₂₁-Gal-DTPA.

Molecules	Chemical Structure	CMC (mM)	a (Å ²)
A		0.016	56
4		0.14 ± 0.04	190 ± 18
4		0.01 ± 0.003	188 ± 20

Gibbs absorption isotherm (Table 1). These values are comparable, independent of the nature of hydrophobic part and very high as compared to precursor like **A** which exhibited an interfacial cross-section of only 56 Å² (see Fig. 1) (Périno et al., 2006). This result supports a presentation of the DTPA moiety in the polar head cross-section and probably an electric repulsion between the carboxylate moieties.

3.3. Size of the particles

The three amphiphiles C₆F₁₃-Gal-DTPA, C₈F₁₇-Gal-DTPA and C₁₀F₂₁-Gal-DTPA were then diluted in H₂O above their critical micellar concentration and their hydrodynamic diameter was measured by dynamic light scattering. They form small particles with a diameter comprised between 10 and 50 nm as shown in Fig. 2. The size of these particles is markedly higher than that of spherical micelles usually obtained with hydrocarbon surfactants and is well correlated with the possible formation of cylindrical micelles or rod-like supramolecular systems as already shown with glycosylated-derived fluorinated surfactants (Lebaupain et al., 2006; Polidori et al., 2006). The fluctuation of the few aggregates in the medium over the time leads to the formation of unstable diffusing objects which gives a strong correlation signal and might influence the data leading to a mistaken value. However, transmission electronic microscopy showed that in terms of number of objects, very few aggregates could be observed indicating a majority of small objects. We can note a decrease of the particle size when increasing the fluorinated tail length. Such a result could be ascribed to an increase of hydrophobic interactions within the fluorinated core of the aggregates. Interestingly, the perfluoroalkyl amphiphiles still form small particles despite the presence of DTPA which represents a large polar head as described above. As the more

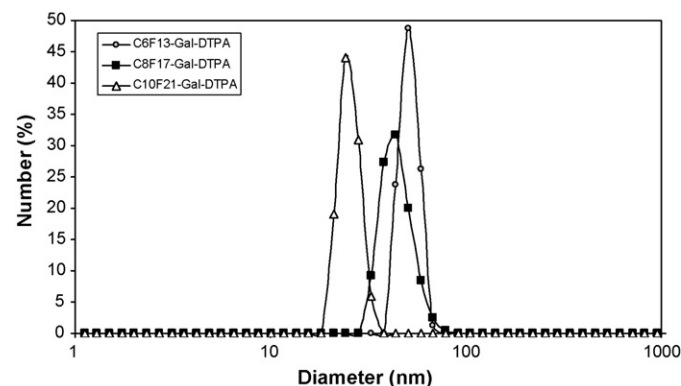


Fig. 2. Size distribution of the amphiphiles bearing a C₆F₁₃, C₈F₁₇ and C₁₀F₂₁ fluorocarbon chain.

homogeneous size distribution was obtained with the compound C₁₀F₂₁-Gal-DTPA, *in vitro* and *in vivo* studies were performed with this molecule.

3.4. Interaction of particles with blood proteins

Before starting the biological studies, we verified that the chemically modified perfluoroalkylated amphiphile (C₁₀F₂₁) bearing a lactosyl group and a DTPA moiety did not interfere with blood components. For this purpose, we complexed the lipid with europium and incubated the micelles formed out of this lipid in serum for 2 h at 37 °C. Then proteins were precipitated and the amount of amphiphile left in the supernatant was evaluated by measuring the retarded fluorescence of the DTPA complexed europium ions. The amount of C₁₀F₂₁-Gal-DTPA recovered in the supernatant corresponded to 82% of the initial quantity, which showed that despite the incorporation of lactosylated and DTPA moieties, the perfluoroalkylated amphiphile interacted poorly with blood proteins.

3.5. Agglutination tests

The results of the agglutination tests using the nanoparticles formed in water using C₁₀F₂₁-Gal-DTPA and ricin RCA120 are reported in Fig. 3. The observed 450 nm diffusion scattering absorption indicated the formation of aggregates between the nanoparticles and ricin. Furthermore, when ricin was first incubated with lactose, the value of the 450 nm absorbance decreased, in a concentration dependent manner. These results indicate that the interaction of ricin with the nanoparticles can be blocked in the presence of lactose, which shows that the galactose ligands are present on the outer surface of the nanoparticles and are responsible for the aggregation in the presence of ricin. This is a crucial point for the further *in vivo* interactions of these nanoparticles with the ASGPR present on the surface of hepatocytes.

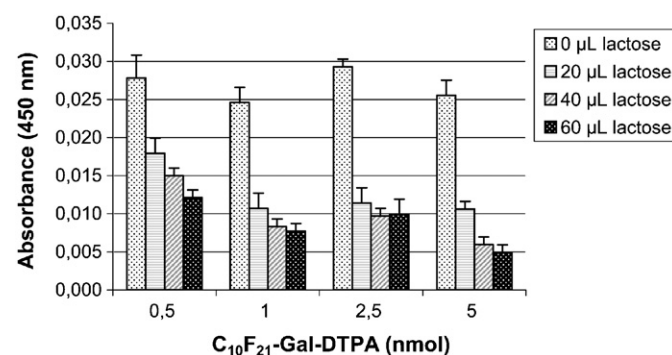


Fig. 3. Agglutination tests using nanoparticles formed with C₁₀F₂₁-Gal-DTPA and RCA120.

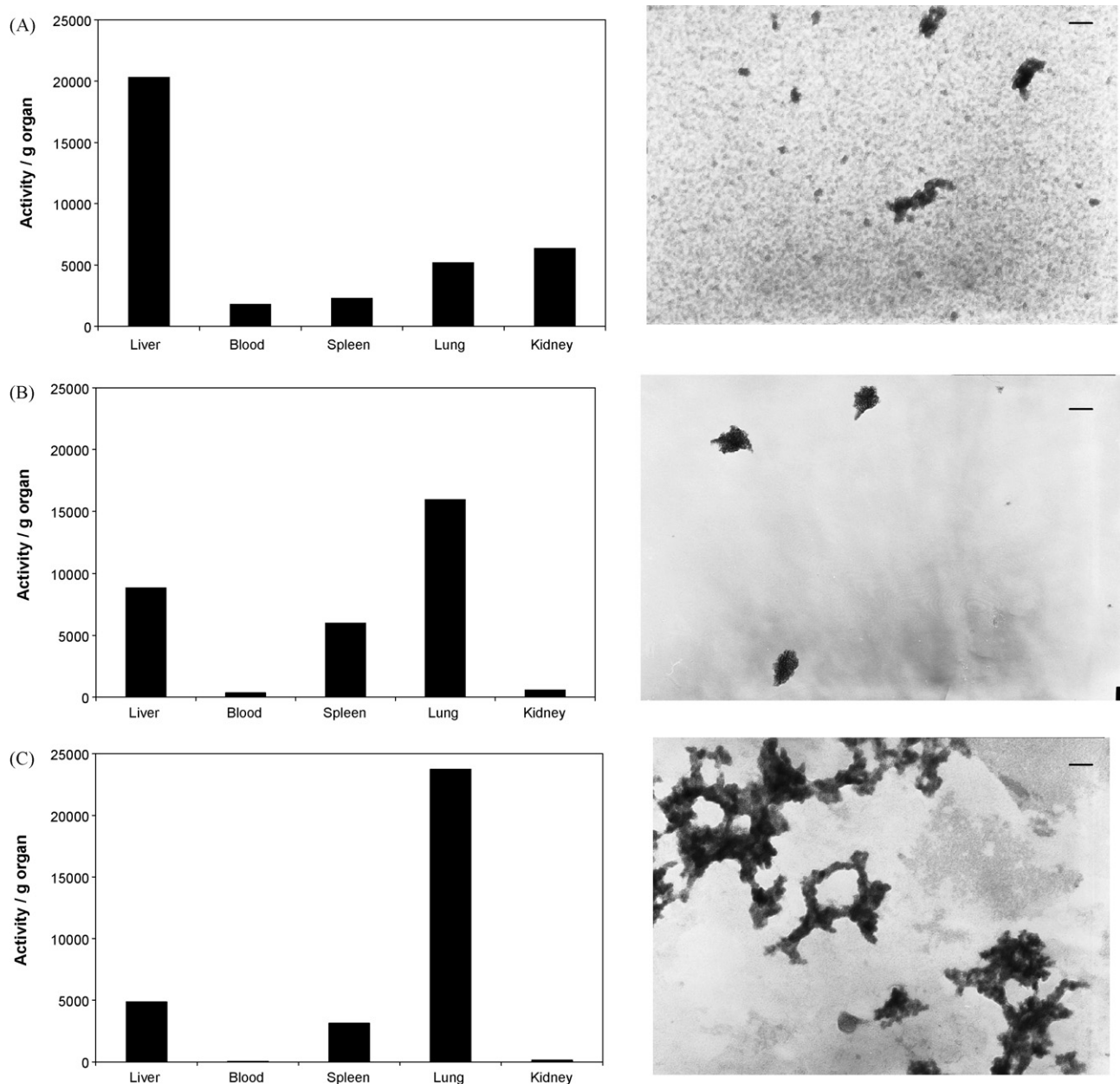


Fig. 4. Results of biodistribution of the nanoparticles labeled with ^{99m}Tc (left) at pH 6 (A, left), pH 5.5 (B, left) and pH 5 (C, left). Corresponding TEM pictures (right) of $\text{C}_{10}\text{F}_{21}\text{-Gal-DTPA}$ dispersed in sodium acetate and increasing amount of SnCl_2 to reach pH=6 (A), pH=5.5 (B) and pH=5 (C). Bar at the upside right represents 100 nm.

3.6. Optimised pH conditions for *in vivo* studies

Scintigraphic experiments with technetium as radiotracer necessitate a step of reduction of ^{99m}Tc -pertechnetate as the oxidation state of technetium in many radiopharmaceuticals is Tc(IV). This step requires stringent acidic conditions in presence of tin chloride, a condition which is not appropriate for our $\text{C}_{10}\text{F}_{21}\text{-Gal-DTPA}$ lipid. Indeed, reduction of the pH from 7 to 2 leads to carboxylate protonation and consequently particle aggregation. Conditions used for ^{99m}Tc -pertechnetate reduction were evaluated on $\text{C}_{10}\text{F}_{21}\text{-Gal-DTPA}$. Various salts with different ionic strength were used in order to maintain the pH above 5 in spite of the presence of tin chloride (SnCl_2) diluted in HCl 0.1 M. Sodium acetate (200 mM), which is widely used as a buffer *in vivo*, was chosen to maintain the pH above 5. Three samples containing increasing amounts of SnCl_2 were prepared. Labeling with ^{99m}Tc was checked by chromatog-

raphy to insure that less than 3% of free ^{99m}Tc would be injected. To optimise the conditions for *in vivo* systemic delivery, the samples were injected intravenously to two rats and particle stability was checked in parallel by transmission electronic microscopy. As can be seen, the sample bearing the less amount of SnCl_2 (pH 6) (Fig. 4A) did exhibit a quite homogeneous size distribution situated between 10 and 20 nm with few aggregates. As the amount of SnCl_2 increased and the pH decreased to 5.5 then 5, more and more aggregates formed (Fig. 4B and C). Injection of these samples to rats showed a major distribution in the liver for the first sample (Fig. 4A), while increasing amounts of the radioactivity was recovered in the lung for the next two samples (Fig. 4B and C). These data appear coherent with the size of the particles. It is well known that large particles are retained in the lung post-bolus injection due to the capillary small diameter. The ratio between liver and lung distribution is in favour of the first sample in which the pH was

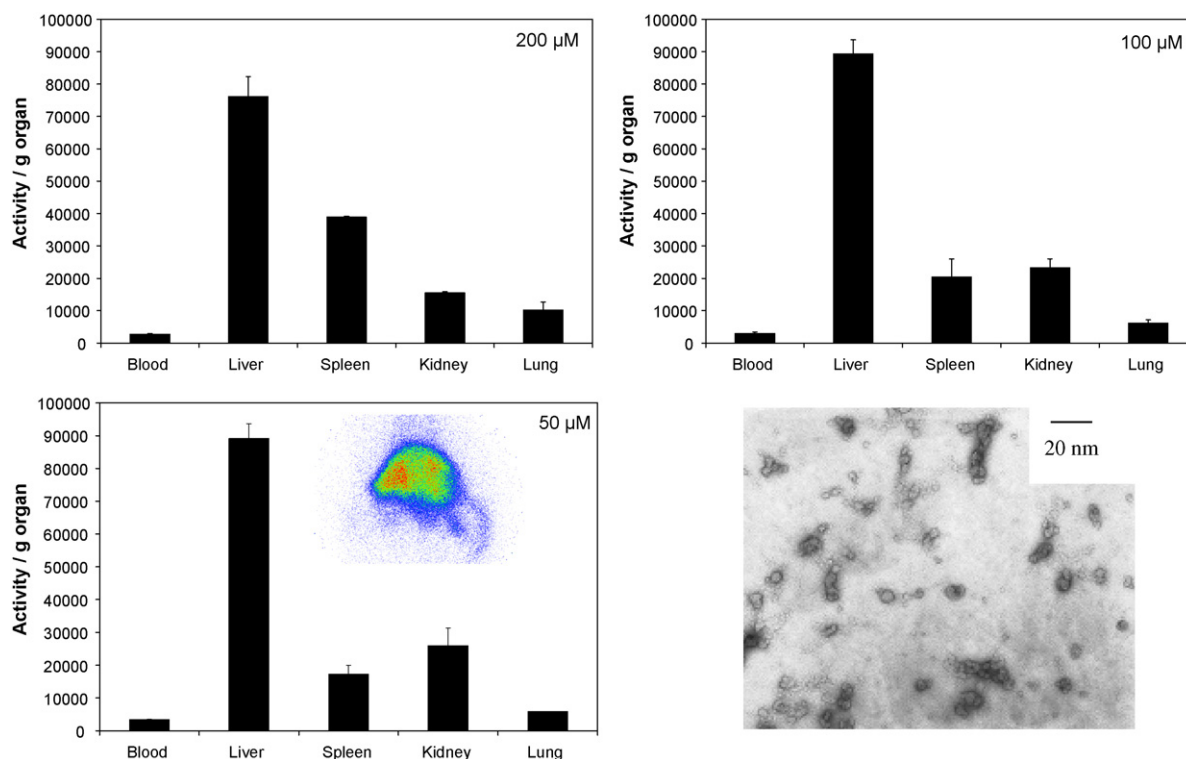


Fig. 5. Results of biodistribution of the nanoparticles labeled with ^{99m}Tc at 200, 100 and 50 μM at pH 6 in two rats. Measured activity per organ (histogram) and corresponding image of scintigraphy at 50 μM (inset). TEM picture of the $\text{C}_{10}\text{F}_{21}$ -Gal-DTPA at 50 μM in H_2O .

maintained at 6 which still allowed ^{99m}Tc -pertechnetate reduction and conservation of the homogeneity of the suspension.

3.7. Optimised concentration for *in vivo* studies

After optimising the pH of the suspension during the labeling process, the concentration of the suspension was studied. Previous experiments were performed at 200 μM $\text{C}_{10}\text{F}_{21}$ -Gal-DTPA to insure the formation of micelles, the critical micellar concentration being measured at 10 μM for $\text{C}_{10}\text{F}_{21}$ -Gal-DTPA. Transmission electronic microscopy images (Fig. 4A) showed that the homogeneity of the suspension was mostly conserved in the conditions used, but could be improved. In order to avoid the formation of the few aggregates observed and improve the liver versus lung accumulation ratio, we used more diluted suspensions. The three following concentrations were used, 50, 100 and 200 μM while maintaining the preparation pH at 6 by keeping the ratio amphiphile to SnCl_2 constant. The biodistribution profile in rats is given in Fig. 5.

At the three tested concentrations, a major accumulation was observed in the liver. The ratio of radioactivity calculated between liver and lung increased by a factor of 2 from concentration 200 to 100 μM . This ratio was similar between concentrations of 100 and 50 μM indicating that the particles were indeed colloiddally stabilised at the concentrations 100 and 50 μM as could also be observed by TEM (Fig. 5, 50 μM). The presence of a signal in the spleen suggested that part of the perfluoroalkyl nanoparticles were taken up by Kupffer cells. However, the calculated ratio between the radioactivity in the liver and in the spleen increased by a factor 2.5 from concentration 200 to 100 μM suggesting that this uptake was favourably reduced even though part of Kupffer cell uptake might subsist. The radioactivity ratio between liver and spleen was similar between concentrations 100 and 50 μM showing that the same liver accumulation occurred for these optimised conditions. The size limit of the objects that can reach the hepatocytes

through the Disse space is unclear. Less than 10 nm diameter is reported to be appropriate and indeed a modified protein bearing a lactosylated ligand was shown to fully distribute to the liver (Scherman et al., 2008). However, bigger size particles have been reported to reach hepatocytes when decorated with asialoglycoprotein receptor ligand (Weeke-Klimp et al., 2007; Kim et al., 2006). A morphological study of the intersinusoidal space by scanning electronic microscopy showed that this zone exhibit extensive ramifications and was described as a labyrinth of intercellular channels (Motta and Porter, 1974) which could explain the passage of different type of particles. In particular, liposomes bearing lactosylated or galactosylated ligands have been shown to reach the hepatocytes (Kawakami et al., 2001) which might be due to their flexible membrane. One has to be prudent on the distribution as reported earlier by Spanjer et al. (1985). Further investigations are required to discriminate how the perfluoroalkyl lactosylated nanoparticles distribute into the liver and in particular if the hepatocyte captation is the main route as desired.

4. Conclusion

Amphiphilic perfluoroalkyl carbohydrates were chosen for their long circulation time due to their poor interaction with blood components and their interaction with asialoglycoprotein receptors to insure an efficient targeting to the liver via the hepatocytes. Despite the introduction of a DTPA moiety, the perfluoroalkylated amphiphiles were still able to form small structures where the lactosylated moiety was exposed at the surface of the nanoparticles as confirmed by agglutination tests with ricin. Conditions of pH, ionic strength and concentrations have been optimised to maintain a homogeneous size distribution with particles in the order of 10–20 nm. Finally, we have shown that, optimising these conditions allowed reducing the lung and spleen captation in favour of liver accumulation.

Acknowledgements

The authors thank the Service Commun d'Imagerie Cellulaire et Moléculaire from the University Paris Descartes and particularly René Lai-Kuen for his help in the TEM experiments.

References

- Abe, M., Lai, J., Kortylewicz, Z.P., Nagata, H., Fox, I.J., Enke, C.A., Baranowska-Kortylewicz, J., 2003. Radiolabeled constructs for evaluation of the asialoglycoprotein receptor status and hepatic functional reserves. *Bioconjug. Chem.* 14, 997–1006.
- Arya, P., Kutterer, K.M.K., Qin, H., Roby, J., Barnes, M.L., Lin, S., Lingwood, C.A., Peter, M.G., 1999. α -Galactose based neoglycopeptides. Inhibition of verotoxin binding to globotriosylceramide. *Bioorg. Med. Chem.* 7, 2823–2833.
- Barthélémy, P., Tomao, V., Selb, J., Chaudier, Y., Pucci, B., 2002. Fluorocarbon–hydrocarbon nonionic surfactants mixtures: a study of their miscibility. *Langmuir* 18, 2536–2557.
- Bedossa, P., Poynard, T., 1996. An algorithm for the grading of activity in chronic hepatitis C. The metavir cooperative study group. *Hepatology* 24, 289–293.
- Burkitt, S.J., Ottewill, R.H., Hayter, J.B., Ingram, B.T., 1987. Small angle neutron scattering studies on micellar systems. Part 1. Ammonium octanoate, ammonium decanoate and ammonium perfluorooctanoate. *Colloid Polym. Sci.* 265, 619–627.
- Child, C.G., Turcotte, J.G., 1964. In: Child, C.G. (Ed.), *The Liver and Portal Hypertension*. Surgery and Portal Hypertension. Saunders, Philadelphia, pp. 50–64.
- Chaubaud, E., Barthélémy, P., Mora, N., Popot, J.-L., Pucci, B., 1998. Stabilization of integral membrane proteins in aqueous solution using fluorinated surfactants. *Biochimie* 80, 515–530.
- Coulon, J., Bonaly, R., Pucci, B., Polidori, A., Barthelemy, P., Contino, C., 1998. Cell targeting by glycosidic telomers. Specific recognition of the Kb CWL1 lectin by galactosylated telomers. *Bioconjug. Chem.* 9, 152–159.
- Curran, D.P., 2003. A bird's eye view of fluororous reaction and separation techniques. *Actualité Chimique* 4–5, 67–71.
- Eckelman, W., 1995. Radiolabeling with technetium-99m to study high-capacity and low-capacity biochemical systems. *Eur. J. Nucl. Med. Mol. Imaging* 22, 249–263.
- Imbert-Bismut, F., Ratziu, V., Pieroni, L., Charlotte, F., Benhamou, Y., Poynard, T., 2001. Biochemical markers of liver fibrosis in patients with hepatitis C virus infection: a prospective study. *Lancet* 357, 1069–1075.
- Hakomori, S.-i., Handa, K., 2000. Glycosphingolipid microdomains in signal transduction, cancer, and development. In: Ernst, B., Hart, G.W., Sinaý, P. (Eds.), *Carbohydrates in Chemistry and Biology Part II*, vol. 4. Wiley-VCH, Weinheim, pp. 771–781.
- Hwang, E.-H., Taki, J., Shuke, N., Nakajima, K., Kinuya, S., Konishi, S., Michigishi, T., Aburano, T., Tonami, N., 1999. Preoperative assessment of residual hepatic functional reserve using ^{99m}Tc -DTPA-galactosyl-human serum albumin dynamic SPECT. *J. Nucl. Med.* 40, 1644–1651.
- Jeong, J.M., Hong, M.K., Lee, J., Son, M., So, Y., Lee, D.S., Chung, J.-K., Lee, M.C., 2004. ^{99m}Tc -neolactosylated human serum albumin for imaging the hepatic asialoglycoprotein receptor. *Bioconjug. Chem.* 15, 850–855.
- Kawakami, S., Munakata, C., Fumoto, S., Yamashita, F., Hashia, M., 2001. Novel galactosylated liposomes for hepatocyte-selective targeting of lipophilic drugs. *J. Pharm. Sci.* 90, 105–113.
- Kissa, E., 1994. *Fluorinated Surfactants: Synthesis, Properties, Applications*. Surfactants Science Series, vol. 50. Dekker, New York (Chapter 7, pp. 264–282).
- Kim, E.-M., Jeong, H.-J., Kim, S.-L., Sohn, M.-H., Nah, J.-W., Bom, H.-S., Park, I.-K., Cho, C.-S., 2006. Asialoglycoprotein-receptor-targeted hepatocyte imaging using ^{99m}Tc galactosylated chitosan. *Nucl. Med. Biol.* 33, 529–534.
- Lebaupain, F., Salvay, A.G., Olivier, B., Durand, G., Fabiano, A.S., Michel, N., Popot, J.L., Ebel, C., Breyton, C., Pucci, B., 2006. Lactobionamide surfactants with hydrogenated, perfluorinated or hemifluorinated tails: physical-chemical and biochemical characterization. *Langmuir* 22, 8881–8890.
- Maurizis, J.-C., Pavia, A.-A., Pucci, B., 1993. Efficiency of non-ionic telomeric surfactants for the solubilization of subcellular fractions proteins. *Bioorg. Med. Chem. Lett.* 3, 161–164.
- Motta, P., Porter, K., 1974. Structure of rat liver sinusoids and associated tissue spaces as revealed by scanning electron microscopy. *Cell Tissue Res.* 148, 111–125.
- Périno, S., Contino-Pépin, C., Jasseron, S., Rapp, M., Maurizis, J.C., Pucci, B., 2006. Design, synthesis and preliminary biological evaluations of novel amphiphilic drug carriers. *Bioorg. Med. Chem. Lett.* 16, 1111–1114.
- Polidori, A., Presset, M., Lebaupain, F., Ameduri, B., Popot, J.-L., Breyton, C., Pucci, B., 2006. Fluorinated and hemi-fluorinated surfactants derived from maltose: synthesis and application to handling membrane proteins in aqueous solution. *Bioorg. Med. Chem. Lett.* 16, 5827–5831.
- Pugh, R.N., Murray-Lyon, I.M., Dawson, J.L., Pietroni, M.C., Williams, R., 1973. Transsection of the oesophagus for bleeding oesophageal varices. *Br. J. Surg.* 60, 646–649.
- Ravey, J.C., Stebe, M.J., Sauvage, S., 1994. Water in fluorocarbon gel emulsions: structures and rheology. *Colloids Surf. A: Physicochem. Eng. Aspects* 91, 237–257.
- Scherman, D., Bessodes, M., Chaumet-Riffaud, P., Mignet, N., 2008. New conjugates for therapeutic purposes and/or as diagnosis and/or imaging agents and method for preparing the same. WO/2008/074960.
- Slidregt, L.A.J.M., Rensen, P.C.N., Rump, E.T., van Santbrink, P.J., Bijsterbosch, M.K., Valentijn, A.R.P.M., van der Marel, G.A., van Boom, J.H., van Berkel, T.J.C., Biessen, E.A.L., 1999. Design and synthesis of novel amphiphilic dendritic galactosides for selective targeting of liposomes to the hepatic asialoglycoprotein receptor. *J. Med. Chem.* 42, 609–618.
- Spanjer, H., Van berkel, T., Scherphof, G., Kempfen, H., 1985. The effect of a water-soluble tris-galactoside terminated cholesterol derivative on the in vivo fate of small unilamellar vesicles in rats. *Biochim. Biophys. Acta* 916, 396–402.
- Von Rybinski, W., Hill, K., 1998. *Angew. Chem. Int. Ed. Engl.* 37, 1328–1345.
- Wang, K., Karlsson, G., Almgren, M., Asakawa, T., 1999. Aggregation behavior of cationic fluorosurfactants in water and salt solutions. A cryo-TEM survey. *J. Phys. Chem. B* 103, 9237–9246.
- Weeke-Klimp, A., Bartsch, M., Morselt, H., Van Veen-Hof, I., Meijer, D., Scherphof, G., Kamps, J., 2007. Targeting of stabilized plasmid lipid particles to hepatocytes in vivo by means of coupled lactoferrin. *J. Drug target.* 15, 585–594.